Progress In Electromagnetics Research C, Vol. 27, 239–252, 2012

COMPACT RECONFIGURABLE UWB ANTENNA INTEGRATED WITH STEPPED IMPEDANCE STUB LOADED RESONATORS AND SWITCHES

Y. S. Li[1,*], W. X. Li[1], and Q. B. Ye[2]

[1]College of Information and Communications Engineering, Harbin Engineering University, Harbin, Heilongjiang 150001, China

[2]Communications Research Centre, 3701 Carling Ave., Ottawa K2H 8S2, Canada

Abstract—A compact reconfigurable antenna integrated with stepped impedance stub (SIS) loaded stepped impedance resonator (SIR) and SIS loaded hexagon stepped impedance resonator (HSIR) for ultra wideband (UWB) applications is proposed in this paper. The reconfigurable UWB antenna can work as a UWB antenna and a dual notch band UWB antenna by controlling the switches ON and OFF. The proposed two notch bands are obtained by embedding a SIS-HSIR on hexagon radiation patch and a SIS-SIR on coplanar waveguide (CPW) excitation line. The reconfigurable characteristic is achieved by means of two ideal switches. The proposed reconfigurable antenna has been designed, fabricated and measured. The experimental results show that the proposed reconfigurable antenna has a multi-mode function and good omni-directional characteristics.

1. INTRODUCTION

The pursuits for high speed data and high efficiency communications have resulted in tremendous amount of research activities in wireless communications community. UWB is a well-known technology with high speed data ratio, low power and high resistance to interference in wireless communication [1]. For these reasons, UWB communication has attracted much attention in recent years. A UWB antenna is an important part in UWB wireless communication, and a lot of UWB antennas have been proposed for UWB applications [2–14]. However,

Received 26 January 2012, Accepted 22 February 2012, Scheduled 28 February 2012

* Corresponding author: Ying-Song Li (liyingsong@hrbeu.edu.cn).

most of the previous UWB antennas have large size and complex structures. Recently, printed wide slot antennas are developed for UWB applications such as rectangular wide slot [4], polygon wide slot [5], circular wide slot [6, 7]. However, some narrow band systems have been used for a long time in UWB band. The existed narrow band systems have potential electromagnetic interference (EMI) with UWB systems. In the conventional design, band-stop filters are added at the end of the antennas or the devices. Thereby, the cost is increased and the size of the antenna is getting large [8]. Designing a UWB antenna with one or several rejection filter characteristics is a hot topic in recent years. Plenty of UWB antennas with notch band characteristics have been developed for these applications [9–14]. However, most of the notch band UWB antennas are formed by etching half wavelength or quarter wavelength slot on radiation patch and ground plane. The embedded slots will leak electromagnetic wave which deteriorates the radiation patterns of notched UWB antennas. An effective technology is to insert open circuited stubs [11, 12] into the UWB antenna and integrate filter [13–15] in the feed line and active region. Some antennas using SRRs in the feed structures [15] are also utilized to avoid the unrequired band. All the methods can achieve a good band notch characteristic, but some of the notched band structures are complex and difficult to design. In addition, the notch depth is poor and the proposed UWB antennas just work in UWB states or notch band UWB states. In this article, a polygon wide slot antenna for reconfigurable UWB communications applications is presented numerically and experimentally. The proposed antenna can be used as a multi-mode antenna, such as a UWB antenna or a dual notch band UWB antenna. The dual notch band functions are obtained by etching a SIS-HSIR in hexagon radiation patch and a SIS-SIR in CPW transmission signal strip line. By adjusting the dimensions of SIS-SIR and SIS-HSIR, the center frequency and bandwidth of the two notch bands can be tuned to meet practical requirement. The reconfigurable characteristic is achieved by using two ideal switches on SIS-HSIR and SIS-SIR. By controlling the switches ON and OFF, the proposed antenna can work as a UWB antenna, a dual notch band antenna/tri-band antenna, a notch band UWB antenna/dual band antenna. Details of the antenna design and both numerical and experimental results are presented and discussed. Good agreement between simulated and measured results demonstrates that the designed antenna is suitable for UWB communications, multi-band communications and notch band UWB communications applications.

2. ANTENNA DESIGN

The configurations of the proposed antennas are shown in Fig. 1. Fig. 1(a) illustrates the geometry of the proposed dual notch band UWB antenna (antenna 1). The notched UWB antenna consists of a polygon wide slot, a hexagon radiation patch, a SIS-HSIR etched inside the hexagon radiation patch, a SIS-SIR embedded in CPW transmission signal strip line and a 50 Ω CPW feed structure. The resonator frequency of the two resonators SIS-HSIR and SIS-SIR can be calculated using resonator theory [16]. First, a wide slot UWB antenna is designed based on previous design proposed in [11]. Then, the calculated two resonators SIS-HSIR and SIS-SIR are etched on hexagon radiation patch and CPW excitation line, respectively. To achieve the reconfigurable functions, two ideal switches are set on SIS-HSIR and SIS-SIR. Fig. 1(b) is the reconfigurable UWB antenna based on the proposed dual notch band UWB antenna 1. The two ideal switches are set on SIS-HSIR and SIS-SIR, respectively. A substrate with relative permittivity of 2.65, a loss tangent of 0.002 and a thickness of $h = 1.6$ mm is used in antenna designs. The SIS-HSIR produces the

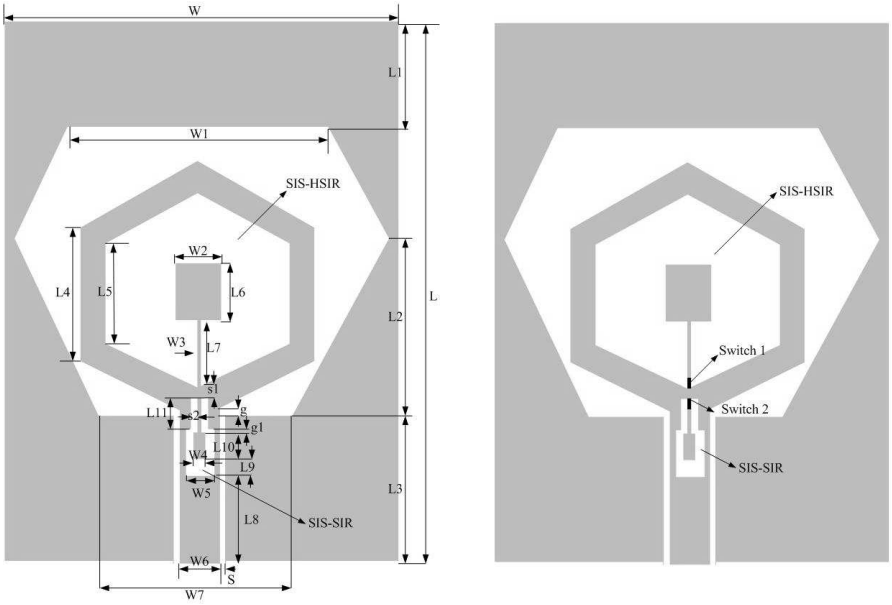

Figure 1. Geometries of the proposed antennas. (a) Dual notch band UWB antenna (antenna1). (b) Reconfigurable UWB antenna (antenna 2).

notch band near 5.5 GHz (lower notch band) and the SIS-SIR gives the notch band near 9 GHz (higher notch band). The two switches control the mode of the proposed reconfigurable UWB antenna. The 50 Ω CPW feed structure consists of the CPW transmission signal strip line with a signal strip width $W_6 = 3.6$ mm, and the gap between the CPW ground plane and transmission signal strip with width $S = 0.2$ mm. The 50 Ω CPW structure of the proposed UWB antenna is designed by using the standard equations [17]. The designed antenna has a compact size which is 32 mm × 24 mm ($L \times W$). In this paper, the proposed antenna is investigated by means of HFSS which is based on the finite element method (FEM). In this paper, the two ideal switches are replaced by two microstrip lines with length 2 mm and width 0.3 mm. During the simulation and measurement, the presence of a metal bridge represents ON state and the absence of a metal bridge represents OFF state [18].

3. SIMULATED AND MEASURED RESULTS AND DISCUSSIONS

According to the rule and theory of SIS-SIR and SIS-HSIR filter [16], the proposed reconfigurable UWB antenna has been optimized using HFSS. Two ideal switches with length 2 mm and width 0.3 mm are employed in simulation and measurement. During the optimization, the presence of a metal bridge represents ON state and the absence of a metal bridge represents OFF state. The optimized dimensions of proposed reconfigurable UWB antenna are as follows: $L = 32$ mm, $W = 24$ mm, $L_1 = 6.4$ mm, $L_2 = 10.2$ mm, $L_3 = 9.4$ mm, $L_4 = 8$ mm, $L_5 = 5.4$ mm, $L_6 = 2.5$ mm, $L_7 = 4.65$ mm, $L_8 = 3.5$ mm, $L_9 = 1.8$ mm, $L_{10} = 1.5$ mm, $L_{11} = 3.3$ mm, $W_1 = 16$ mm, $W_2 = 2$ mm, $W_3 = 0.3$ mm, $W_4 = 2$ mm, $W_5 = 2.9$ mm, $W_6 = 3.6$ mm, $W_7 = 13.8$ mm, $S = 0.2$ mm, $g = g_1 = 0.2$ mm, $s_1 = 0.4$ mm, $s_2 = 0.25$ mm. The SIS-HSIR and SIS-SIR play an important effect on notch band characteristics and reconfigurable functions. So, the parameters of SIS-HSIR and SIS-SIR are investigated and discussed herein. During the investigation, one parameter is changed with other parameters fixed.

3.1. The Length L_6 of SIS-HSIR

Figure 2 illustrates the simulated return losses of antenna 1 as a function of frequency for the different values of L_6. It can be seen from Fig. 2 that the lower notch band moves to low frequency with the increasing of L_6 and the higher notch band remains unchanged. In addition, the impedance bandwidth ranging from 5.4 GHz to 7.8 GHz

is improved. This is caused by the increased L_6 which changes the characteristic impedance and electrical length of SIS-HSIR.

3.2. The Width W_2 of SIS-HSIR

Figure 3 shows the simulated return losses of the proposed antenna 1 in terms of W_2. From Fig. 3, we can see that the lower notch band moves to the low frequency and the impedance bandwidth at the low frequency is getting worse. However, the impedance bandwidth from 5.3 GHz to 7.8 GHz is also improved. In this investigation, the higher notch band is almost fixed. This is due to the increased width W_2 which alters the coupling between the stepped impedance stub of SIS-HSIR and hexagon impedance resonator.

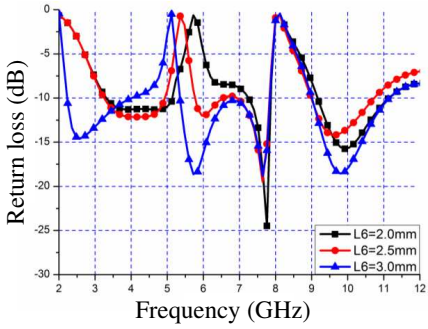

Figure 2. Effects of L_6.

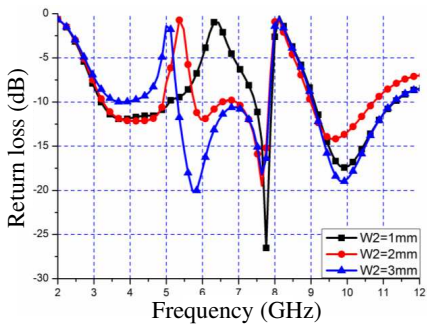

Figure 3. Effects of W_2.

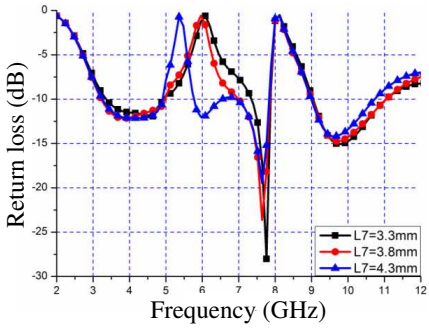

Figure 4. Effects of L_7.

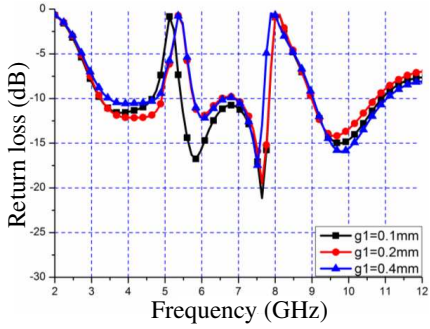

Figure 5. Effects of coupling gap g_1.

3.3. The Length L_7 of SIS-HSIR

Figure 4 demonstrates the return losses of antenna 1 by increasing the length of L_7. It is found that the center frequency of the lower notch band also moves to the low frequency, while higher notch band is constant. In addition, the impedance bandwidth of the dual notch band antenna has been improved. The increased L_7 changes the characteristic impedance and electrical length of stepped impedance stub of SIS-HSIR, which alters the resonance frequency of SIS-HSIR.

3.4. The Coupling Gap g_1 of SIS-SIR

Figure 5 illustrates the simulated return losses of coupling gap g_1 varying from 0.1 mm to 0.4 mm. It can be seen from Fig. 5 that the notch band bandwidth and the center frequency of the two notch bands can be adjusted by changing coupling gap g_1. However, the coupling gap g_1 also deteriorates the impedance bandwidth of the proposed antenna.

3.5. The Length L_{10} of SIS-SIR

Figure 6 gives the simulated return losses of antenna 1 with various L_{10}. The higher notch band moves to the low frequency by the increase of L_{10}. The bandwidth of the higher notch band is also broadened. The lower notch band changes a little. When $L_{10} = 1$ mm, the lower notch band can reduce potential EMI from wireless area local network (WLAN) and worldwide interoperability microwave access (WiMAX) ranging from 5 GHz to 6 GHz. However, the impedance bandwidth is getting worse with the increase of L_{10}. The higher notch band can be adjusted by choosing proper L_{10} to meet the practical requirement of our project.

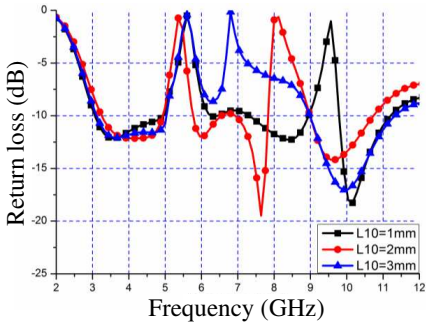

Figure 6. Effects of L_{10}.

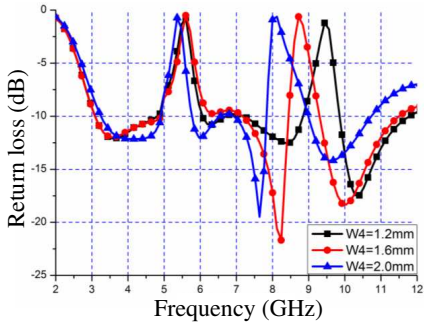

Figure 7. Effects of W_4.

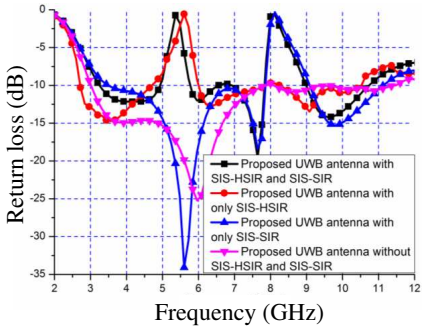

Figure 8. Notch band characteristics of proposed antenna 1.

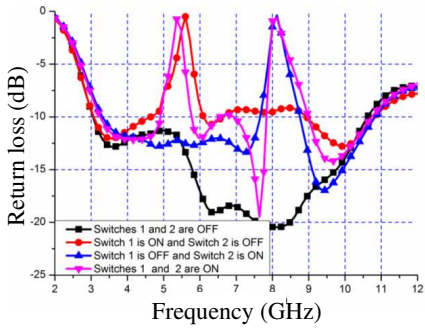

Figure 9. Switch characteristics of proposed antenna 2.

3.6. The Width W_4 of SIS-SIR

Figure 7 shows the return losses characteristics by changing the dimension of W_4. From Fig. 7, the higher notch band moves to low frequency by the increase of W_4. The increased W_4 alters the coupling between stepped impedance stub and stepped impedance resonator. The changed coupling also alters the distributed capacitance and distributed inductance of SIS-SIR. Therefore, the resonance frequency of the SIS-SIR has been changed.

3.7. Notch Band Characteristics of Antenna 1

Figure 8 illustrates the notch band characteristics of antenna 1. It is found that the two notch band functions are obtained by employing the SIS-HSIR and SIS-SIR. The lower notch band is produced by SIS-HSIR and the higher notch band is given by SIS-SIR. According to the study shown in Fig. 8, the proposed two notch band can be design independently. Though the proposed antenna 1 can have two notch bands functions, the impedance bandwidth is getting a little narrower. This is caused by the etched SIS-HSIR and SIS-SIR which alter the surface current distributions of antenna 1.

3.8. Reconfigurable Characteristics of Antenna 2

Figure 9 expounds the reconfigurable characteristics of the proposed antenna 2. Antenna 2 has the same dimensions as antenna 1. From Fig. 9, we can see that when the two switches are OFF, antenna 2 is a UWB antenna which can cover the whole UWB band ranging from 3.1 GHz to 10.6 GHz. If the two switches are ON, the proposed antenna is a dual notch band UWB antenna which is studied above. While the

switch 1 (SW1) is ON and the switch 2 (SW2) is OFF, the proposed antenna 2 has a notch band between 5 GHz and 6 GHz. If the switch 1 is OFF and the switch 2 is ON, the proposed antenna 2 has a notch band near 8.4 GHz. Therefore, the proposed reconfigurable antenna 2 can be controlled by using two ideal switches on the dual notch band UWB antenna 1. The reconfigurable antenna 2 can be regarded as a UWB antenna by turning the two switches OFF. And antenna 2 can be used as a notch band UWB antenna or a dual band antenna by controlling one switch ON and the other switch OFF. When the two stitches are ON, the antenna is a dual notch band UWB antenna or a tri-band antenna for multi-band wireless communication applications. So, the proposed antenna is a multi-mode antenna which can be used as a UWB antenna, a dual notch UWB antenna/tri-band antenna, a notch band UWB antenna/ dual band antenna. The proposed antenna has a tunable notch band characteristics and a reconfigurable characteristic which can meet the requirements of multi-mode wireless communication applications.

3.9. Current Distributions of Proposed Reconfigurable Antenna

Figure 10 expands the current density distribution of the proposed reconfigurable UWB antenna. The left of Figs. 10(a)–(d) are the simulated current at 5.5 GHz and the right ones are the current distributions at 8.8 GHz. Fig. 10(a) shows the current distributions of the reconfigurable antenna 2 with both switches ON. It is found that the current mainly flow the SIS-HSIR at 5.5 GHz. The current distributions mainly focus on the SIS-SIR at 8.8 GHz. The strong currents excite the two notch band. The current on the CPW ground plane and hexagon radiation patch is small. Fig. 10(b) demonstrates the current density distribution of the reconfigurable antenna 2 with both switches OFF. It can be seen form Fig. 10(b) that the strong current mainly flow the CPW feed structure and the hexagon radiation patch. The currents on the resonators are small. The current density distributions of the reconfigurable antenna 2 with SW1 ON and SW2 OFF are shown in Fig. 10(c). From Fig. 10(c), we can see that the current mainly focus on the SIS-HSIR at 5.5 GHz and the current mainly flow along the CPW feed structure and the hexagon radiation patch at 8.8 GHz. Therefore, the lower notch band is excited by the strong current on SIS-HSIR. Fig. 10(d) illustrates the current density distribution of the reconfigurable antenna 2 with SW1 OFF and SW2 ON. The strong current flows along the SIS-SIR which produces the higher notch band. The current at 5.5 GHz mainly focus on CPW feed structure.

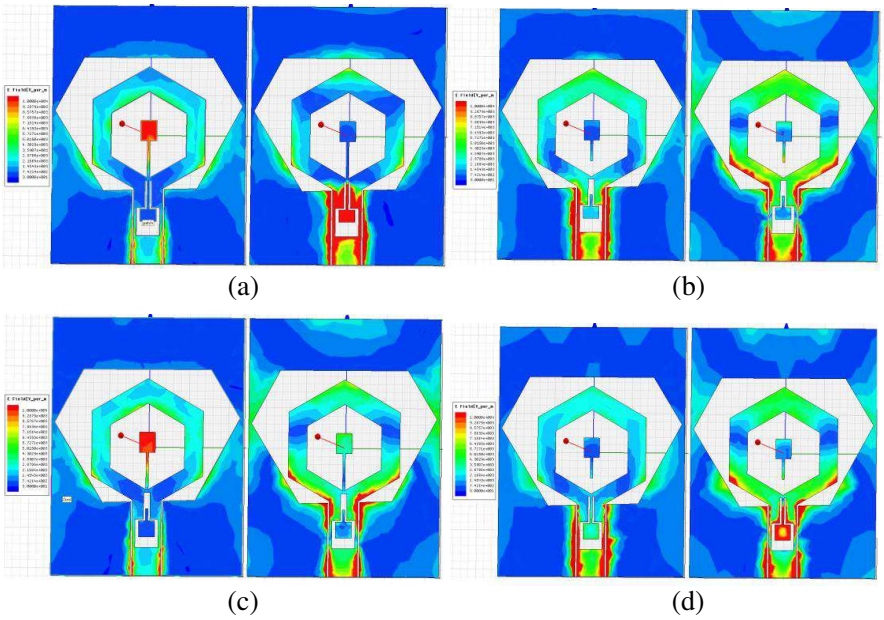

Figure 10. Current distribution of proposed reconfigurable antenna. (a) Antenna 2 with both switches ON. (b) Antenna 2 with both switches OFF. (c) Antenna 2 with SW1 ON and SW2 OFF. (d) Antenna 2 with SW1 OFF and SW2 ON.

3.10. Measured Results and Analysis

To evaluate the performance of the optimized antenna 1 and antenna 2 with two switches OFF, the proposed antennas are fabricated and tested. In this paper, antenna 1 is the reconfigurable antenna 2 with two switches ON. The measured return losses of the proposed antennas are obtained by using Anritsu 37347D vector network analyzer. The photographs of the proposed antennas are shown in Fig. 11. The simulated and measured return losses of the reconfigurable antenna 2 with two switches ON and reconfigurable antenna 2 with two switches OFF are shown in Fig. 12. In order to compare, the simulated return losses of reconfigurable antenna 2 with one switch ON and the other switch OFF are also plotted in Fig. 12.

From Fig. 12, the measured results agree well with the simulated ones which help to verify the accuracy of the simulations. The differences between the simulated and measured values may be due to the errors of the manufactured antenna and the SMA connector to CPW-fed transition, which is included in the measurements but

not taken into account in the calculated results. It is found that the two notch bands are obtained by using SIS-HSIR and SIS-SIR. The proposed reconfigurable antenna 2 with two switches OFF has an impedance bandwidth of 8.1 GHz ranging from 2.9 GHz to 11 GHz. When the two switches are ON, antenna 2 is a dual notch band antenna or a tri-band antenna. The notch band near 5.5 GHz is produced by the upper SIS-HSIR and the 8.8 GHz notch band is provided by SIS-SIR. In this paper, when one of the switches is ON and the other is OFF, the reconfigurable antenna 2 is a notch band UWB antenna or a dual band antenna. The lower notch band is controlled by SIS-HSIR and switch 1. The higher notch band is controlled by SIS-SIR and switch 2.

The measured radiation patterns at 4.0 GHz, 7.0 GHz, 10.0 GHz are shown in Fig. 13. Fig. 13 shows that the antenna can give a nearly omni-directional characteristic in the H-plane and quasi omni-directional pattern in the E-plane. As can be seen from Fig. 13, the radiation patterns in the E-plane deteriorate more or less with the increase of frequency, but the radiation patterns are still nearly quasi omni-directional. The radiation patterns of reconfigurable antenna 2 with two switches ON are worse than those of reconfigurable antenna 2 with two switches OFF. This is caused by the two resonators which leak electromagnetic wave. The leaked electromagnetic wave deteriorates the radiation patterns. The measured peak gains of the proposed antenna at these frequencies are achieved by comparing to a double ridged horn antenna. A stable gain can be obtained throughout the operation band except the notched frequencies. In this paper, the reconfigurable antenna 2 with two switches ON and the reconfigurable

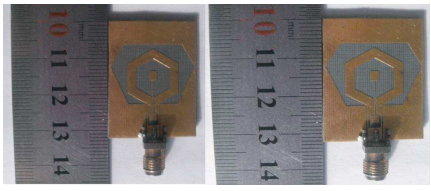

Figure 11. Photograph of proposed reconfigurable antennas. (a) Antenna 1. (b) Antenna 2 with two switches OFF.

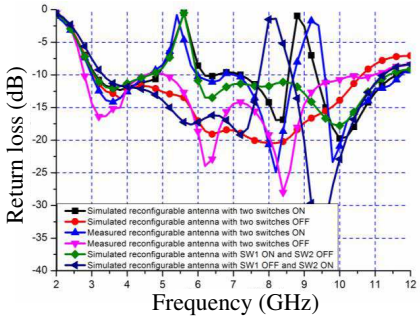

Figure 12. Return losses of proposed reconfigurable UWB antenna.

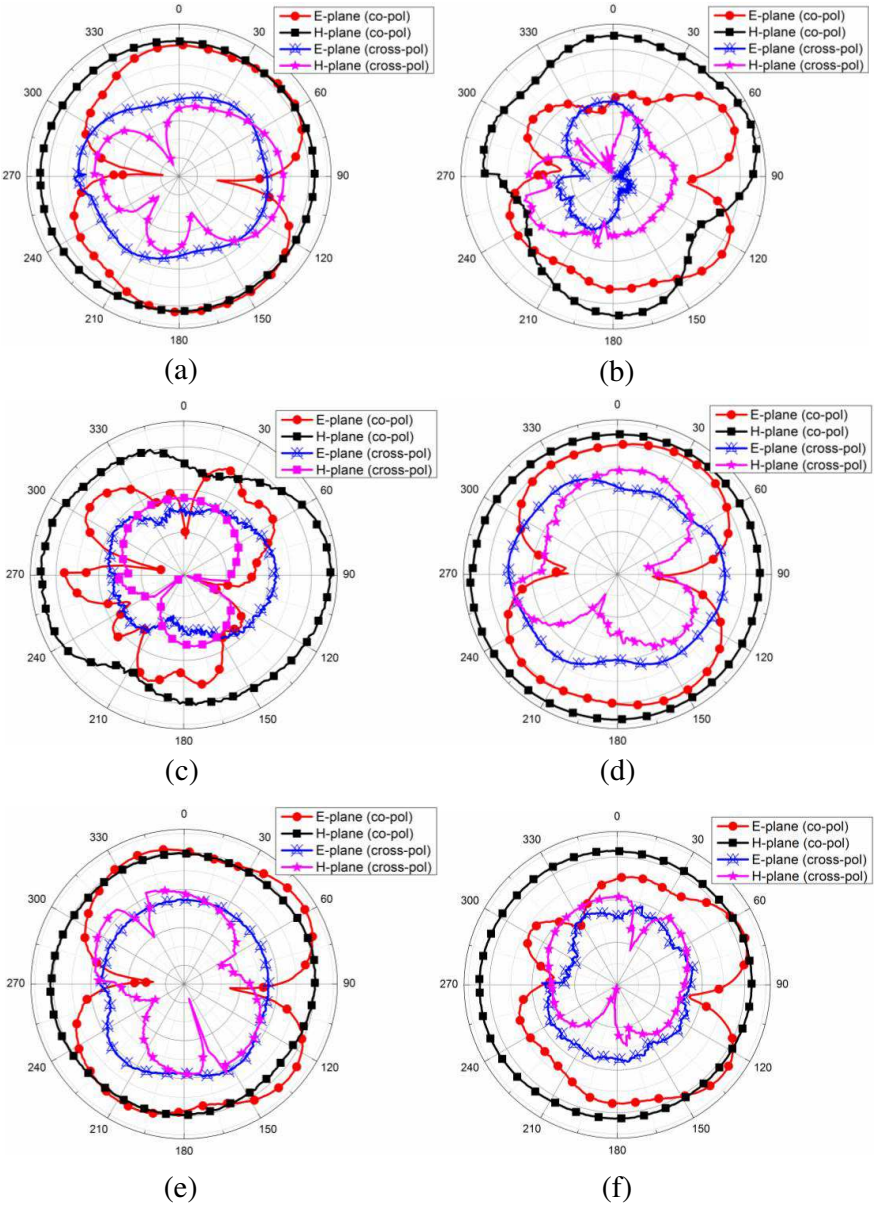

Figure 13. Radiation patterns of proposed reconfigurable antennas. (a) Two switches ON at 4 GHz. (b) Two switches ON at 7 GHz. (c) Two switches ON at 10 GHz. (d) Two switches OFF at 4 GHz. (e) Two switches OFF at 7 GHz. (f) Two switches OFF at 10 GHz.

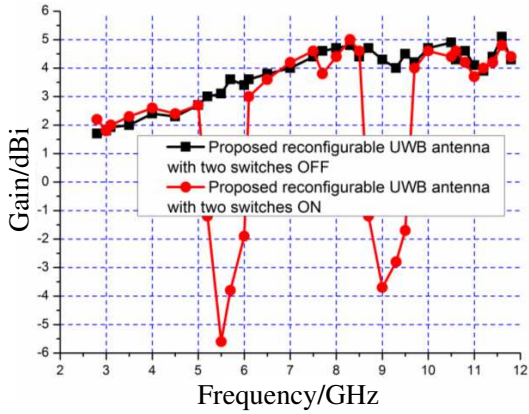

Figure 14. Measured gains of proposed antennas.

antenna 2 with two switches OFF are fabricated and measured. The measured peak gains are shown in Fig. 14. The measured gain of the proposed reconfigurable antenna 2 with two switches OFF is increased from 1.8 dBi to nearly 5.0 dBi which is caused by the deteriorated radiation patterns of the proposed antenna at the high band. In the operation band, the proposed reconfigurable antenna 2 with two switches OFF has stable gains with fluctuation less than 3.2 dBi. But the gain of the proposed reconfigurable antenna 2 with two switches ON dropped quickly from 5.0 GHz to 6.2 GHz and from 8.7 GHz to 9.5 GHz. As desired, two sharp gains decrease in the vicinity of 5.5 GHz and 9 GHz. The gains drop deeply to −5.6 dBi at the lower notch band and −3.8 dBi at the higher notch band.

4. CONCLUSIONS

A reconfigurable UWB antenna using SIS-HSIR, SIS-SIR and two ideal switches is studied numerically and experimentally. The notch band characteristics are obtained by using SIS-HSIR and SIS-SIR. The reconfigurable function is achieved by employing two switches. The proposed reconfigurable UWB antenna can work in UWB mode, dual notch band UWB mode, tri-band mode, and dual band mode. The reconfigurable antennas with two switches ON and OFF are fabricated and measured. The proposed antenna has a small size of 32 mm × 24 mm. Measured and simulated results have good omni-directional radiation patterns, switchable characteristic and good notch band characteristic. The proposed antenna can be suitable for multi-mode wireless communications applications.

ACKNOWLEDGMENT

This work was supported by a grant from the National Defense "973" Basic Research Development Program of China (No. 6131380101). This paper is also supported by the National Natural Science Fundation of China (No. 60902014), Natural Science Fundation of Heilongjiang (QC2009C66). The authors are also thankful to Hebei VSTE Science and Technology Co., Ltd. for providing the measuring facility. The authors are indebted to the editor and to the three anonymous reviewers who gave us many useful comments and constructive suggestions to improve this paper.

REFERENCES

1. Liang, J., C. C. Chiau, X. Chen, and C. G. Parini, "Study of a printed circular disc monopole antenna for UWB system," *IEEE Trans. Antennas Propag.*, Vol. 53, 3500–3504, 2005.
2. Chen, D. and C.-H. Cheng, "A novel compact ultra-wideband (UWB) wide slot antenna with via holes," *Progress In Electromagnetics Research*, Vol. 94, 343–349, 2009.
3. Fallahi, R., A. A. Kalteh, and M. G. Roozbahani, "A novel UWB elliptical slot antenna with band-notched characteristics," *Progress In Electromagnetics Research*, Vol. 82, 127–136, 2008.
4. Li, Y. S., X. D. Yang, C. Y. Liu, and T. Jiang, "Compact CPW-fed ultra-wideband antenna with band-notched characteristics," *Electronics Letters*, Vol. 46, No. 14, 1533–1534, 2010.
5. Ye, L. H. and Q. X. Chu, "3.5/5.5 GHz dual band notch ultra wideband slot antenna with compact size," *Electronics Letters*, Vol. 46, No. 5, 325–327, 2010.
6. Barbarino, S. and F. Consoli, "UWB circular slot antenna provided with an inverted-l notch filter for the 5 GHz WLAN band," *Progress In Electromagnetics Research*, Vol. 104, 1–13, 2010.
7. Gao, G.-P., M. Li, S.-F. Niu, X.-J. Li, B.-N. Li, and J.-S. Zhang, "Study of a novel wideband circular slot antenna having frequency band-notched function," *Progress In Electromagnetics Research*, Vol. 96, 141–154, 2009.
8. Li, Y. S., X. D. Yang, Q. Yang, and C. Y. Liu, "Compact coplanar waveguide fed ultra wideband antenna with a notch band characteristic," *AEU-Int. J. Electron. C*, Vol. 65, 961–966, 2011.
9. Sim, C. Y. D., W. T. Chung, and C. H. Lee, "A circular disc monopole antenna with band rejection function for ultrawideband

application," *Microwave Opt. Technol. Lett.*, Vol. 51, 1607–1613 2009.

10. Danesfahani, R., L. Asadpor, and S. Soltani, "A small UWB CPW-fed monopole antenna with variable notched bandwidth," *Journal of Electromagnetic Waves and Applications*, Vol. 23, Nos. 8–9, 1067–1076, 2009.
11. Li, Y.-S., X.-D. Yang, C.-Y. Liu, and T. Jiang, "Analysis and investigation of a cantor set fractal UWB antenna with a notch-band characteristic," *Progress In Electromagnetics Research B*, Vol. 33, 99–114, 2011.
12. Taheri, M. M. S., H. R. Hassani, and S. M. A. Nezhad, "UWB printed slot antenna with bluetooth and dual notch bands," *IEEE Antennas Wireless Propag. Lett.*, Vol. 10, 255–258, 2011.
13. Djaiz, A., M. Nedil, M. A. Habib, and T. A. Denidni, "Design of a new UWB integrated antenna filter with a rejected WLAN band at 5.8 GHz," *Microwave Opt. Technol. Lett.*, Vol. 53, 1298–1302, 2011.
14. Zhu, Y., F. S. Zhang, R. Zou, Y. C. Jiao, and Q. C. Zhou, "Compact ultra wideband monopole antenna with novel filter," *Journal of Electromagnetic Waves and Applications*, Vol. 25, Nos. 14–15, 2066–2075, 2011.
15. Lui, W. J., C. H. Cheng, and H. B. Zhu, "Improved frequency notched ultrawideband slot antenna using square ring resonator," *IEEE Trans. Antennas Propag.*, Vol. 55, 2445–2450, 2007.
16. Makimoto, M. and S. Yamashita, *Microwave Resonators and Filters for Wireless Communication: Theory, Design And Application*, Springer, 2001.
17. Garg, R., P. Bhartia, I. Bahl, and A. Ittipiboon, *Microstrip Antenna Design Hand Book*, 1st Edition, 794–795, Artech House, 2001.
18. Hamid, M. R., P. S. Hall, P. Gardner, and F. Ghanem, "Switched WLAN wideband tapered slot antenna," *Electronics Letters*, Vol. 46, No. 1, 23–24, 2010.